

## Adsorption Ability of Bagasse Lignin (LB), Bagasse Lignin Carbon (LBF), and Amination Lignin (LA) for Chrome (III)

Nila Tanyela Berghuis\*, Nurul Fitri Novianti, Paramita Jaya Ratri  
Department of Chemistry, Universitas Pertamina, Jl. Teuku Nyak Arief, RT.7/RW.8, Simprug, Kec. Kebayoran Lama, South Jakarta City, 12220.

\*E-mail: [nila.tanyela@universitaspertamina.ac.id](mailto:nila.tanyela@universitaspertamina.ac.id)

DOI: <https://doi.org/10.26874/jkk.v6i1.201>

Received: 11 Jan 2023, Revised: 17 Feb 2023, Accepted: 24 Feb 2023, Online: 29 May 2023

### Abstract

Analyzing the Cr(III) adsorption properties of bagasse lignin (LB), bagasse lignin carbon (LBF), and lignin amine (LA). Variable adsorption studies were performed, including variations in mass, contact time, and pH. The adsorption ability test was carried out first by varying the mass of the adsorbent to determine the optimum mass of each adsorbent LB, LBF, and LA for the Cr(III) adsorbate. The ability of lignin adsorbents (LB, LBF, and LA) to adsorb Cr(III) was optimum at 0.015 g adsorbent mass contact time of 90 minutes, and the adsorbate solution had a pH of 6. The adsorption capacity ( $Q_m$ ) value for bagasse lignin adsorbent (LB) was 8.6050 mg/g at 30°C, bagasse carbon lignin (LBF) was 9.8717 mg/g (30°C), and ammine lignin (LA) with the highest value is 9.9800 mg/g (35 °C).

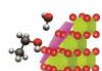
Keywords: adsorption, adsorption kinetics, lignin modification, Cr(III) ion.

### 1 Introduction

In recent years, low-cost and high-performance properties of adsorbents have become a strong demand in adsorbent preparation. Progressive increases in industrial activity produce large amounts of toxic compounds. Many different types of adsorbents may be evaluated to remove pollutants in water especially heavy metals [1]. It is possible to find a large variety of pollutants in waters, mainly of anthropogenic origin, that include pharmaceuticals, toxic metals and metalloids, pesticides, surfactants, and dyes, among others [2,3]. Heavy metals and metalloids are a class of metals that have atomic numbers above 20, and densities over 5 g/cm<sup>3</sup>. Despite some heavy metals and metalloids are a natural part of the environment and fulfill a biological function, almost all heavy metals are toxic to human beings even at low concentrations [4,5]. These metals and metalloids include Cu, Cd, Zn, Cr, As, B, Co, Ti, Sr, Sn, V, Ni, Mo, Hg, Pb, etc [6]. For instance, the leather tanning and electroplating processes generate a mass of chromium ions including Cr(III) and Cr(VI) ions,

which cause high concentrations of Cr(VI) in waters [7]. There are different treatment methods for the removal of toxic metals from water and wastewater, including chemical precipitation, chemical coagulation and flocculation, electrochemical methods, membrane filtration, ion exchange, bioremediation, and adsorption [8]. Among these treatment methods, the adsorption process is considered one of the most effective for water treatment.

The adsorption process can occur between different interfaces such as liquid-solid, liquid-liquid, and physisorption or chemisorption interactions is possible [9]. Adsorption has been the method of choice for heavy metal removal due to its simplicity, high efficiency, adaptability, and sensitivity to plenty harmful metals. Therefore, the design of improved sorbent materials for handling water containing toxic metal ions is imperative. Several parameters, such as high and fast sorption rate, regeneration, reuse, and likewise low creation of toxic residues after deactivation, it has to be met by the sorbent materials [10,11]. Various types of



sorbents, including activated carbon, silica gel, clay minerals, fly ash, and agricultural solid wastes, have been employed as sorbents for the removal of metal ions from wastewater [12]. Activated carbon is one of the most widely used adsorbents owing to its excellent adsorption properties that can remove a wide range of contaminants. However, despite the efficiency of activated carbons, their uses are limited due to their expensive nature [13,14]. In the last decades, biopolymers have attracted much attention as an eco-friendly alternative for heavy metal removal due to their low cost and high availability [15].

Lignin is an amorphous biopolymer and one of the most abundant on the planet. It has carboxyl groups and phenolic units in its macromolecular structure, capable of interacting with metal ions. Lignin can be chemically and physically modified to obtain new materials with improved properties, such as lignin amination and carbonization of lignin [16]. Because of the need for renewable biodegradable resources as raw material to produce adsorbent polymers, lignin has emerged as a good alternative to natural biopolymers due to its great availability, stability, low cost, biodegradability, and CO<sub>2</sub> neutral [17]. Owing to its random polymerization, lignin adopts complex 3D structures with different types of functionalities that depend on their original plants [18]. When lignin and lignin-based polymers are used for heavy metal removal, a high affinity and removal efficiency have been demonstrated, which is attributed to the presence of carboxylic groups and phenolic units in the lignin structure. This makes the use of lignin an eco-friendly and efficient approach for metal adsorbents in water treatment [19].

There are many reviews on the obtention, modification, and synthesis of lignin-containing polymers and nanomaterials and the different uses of lignin and lignin-base materials. However, considering the importance that lignin-based materials have triggered in the last years, and the need to develop new metal sorbent materials, this review focuses for the first time on a comprehensive compilation of the current literature on the use of lignin and lignin-based polymers as sorbents for heavy metals removal on wastewater purification. So, the objective of this work has been to study the adsorption of Cr(III) by using lignin from bagasse, lignin carbonized, and lignin-amine.

## 2 Methods

### 2.1 Materials and Instrumentation

Sugarcane bagasse (PT Indolampung Perkasa), NaOH *p.a* (Merck KGaA), H<sub>2</sub>SO<sub>4</sub> *p.a* (Merck); HCl 37% (Merck), C<sub>2</sub>H<sub>4</sub>(NH<sub>2</sub>)<sub>2</sub> (s) *p.a* (Aldrich KGaA), CH<sub>2</sub>O *p.a* (Merck KGaA), K<sub>2</sub>Cr<sub>2</sub>O<sub>7</sub> (s) *p.a* (Merck KGaA), CH<sub>3</sub>OH (aq) *p.a* (Merck KGaA), and C<sub>9</sub>H<sub>6</sub>O<sub>4</sub>(s) *p.a* (Merck KGaA). All other chemicals and reagents used in this study were: analytical grade and used without further purification. Instrumentation. A Thermo Scientific Genesys 10S has been used for UV-Vis spectroscopy, a Thermo Scientific Nicolet iS5 was used for FTIR in the range of 400-4000 cm<sup>-1</sup>.

Alkali Lignin-bagasse (LB) was isolated from Sugarcane bagasse (PT Indolampung Perkasa) with base methods using 15% NaOH and H<sub>2</sub>SO<sub>4</sub> 5N. Lignin carbon (LBF) was synthesized in the furnace at 500°C for 1 hour. And Lignin-amine was synthesized using methods of Mannich reaction referring to the research of Yuanyuan Ge et al. in 2014 [20].

### 2.2 Characterization of Lignin

All Lignin modifications characterization were studied using FTIR and SEM. FTIR spectroscopy using plat KBr. FTIR all lignin modifications testing was performed at 4000-400 cm<sup>-1</sup>, while SEM lignin morphology was extended to 20 μm.

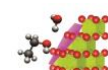
### 2.3 Adsorption Capability

#### 2.3.1 Test for Mass Variation

Each Erlenmeyer flask recently received 15 mg, 30 mg, 45 mg, 60 mg, 75 mg, and 90 mg of lignin. Add Cr metal solution. Using an incubator shaker, stir the mixture at a speed of 250 rpm for 30 minutes. UV-Vis spectroscopy at a wavelength of 440 nm to measure the solution after it was filtered. The optimum mass was established for different contact times. Measurement results are recorded and checked.

#### 2.3.2 Contact Time Variations

Lignin is weighed according to the optimum mass obtained previously and put into an Erlenmeyer, add 10 mL of Cr metal solution. Stirred using an incubator shaker at 250 rpm for 15 each; 30; 45; 60; 75, and 90 minutes. Then filtered, and the solution was measured using UV-Vis spectroscopy at a wavelength of 440nm. For pH variations, the optimum contact time gets reused. The results of the measurements are recorded and examined.



### 2.3.3 Variation of pH

Chromium metal solution is adjusted to the pH value in the range of 1-8 by adding 0.1 M HCl or 0.1 M NaOH. Cr metal solution at each pH was pipetted into an Erlenmeyer containing lignin. Stirring was carried out using an incubator shaker at a speed of 250 rpm during the previously obtained contact time. Then filtered, and the solution was measured using UV-Vis spectroscopy at a wavelength of 440 nm. The measurement results are recorded and analyzed.

## 3 Result and Discussion

### 3.1 Characterization of Lignin

The method of isolating lignin from bagasse refers to the research by Saleh Al Arni in 2018

[21]. Bagasse lignin yielded 3.051 g (6.10%). The yield percentage produced is not much different from the previous by Moubarik et al. in 2013 was 6.2% [22]. This sugarcane bagasse lignin carbonization refers to Gustan Pari et al. in 2006 [23]. The synthesis of amination lignin through the Mannich reaction with the reflux method refers to the research of Yuanyuan Ge et al. in 2014 [20]. The difference is in the source of the amine, which was methylamine in the prior investigation, and ethylenediamine in this study. The synthesis procedure yielded 13.4929 g (67.5 %). Characterization of Lignin modifications based on FTIR spectrum analysis showed the presence of several sharp valleys, which are characteristic of their constituent functional groups.

**Table 1.** FTIR Analysis Results of Bagasse Lignin (LB), Carbonized Lignin (LBF), and Aminated Lignin (LA)

Vibration	Wave number (cm <sup>-1</sup> )			
	Standard Alkaline Lignin	Sugarcane Bagasse Lignin (LB)	Carbonized Lignin (LBF)	Lignin-Amine (LA)
O-H Phenol (Stretching)	3430	3450	-	3390
N-H Amine (Stretching)	-	-	-	3230
C-H Aliphatic (Stretching)	2931	2930	1114	2940
C=C Aromatic (Stretching)	1592	1520	1595	1510
C-N Amine (Stretching)	-	-	-	1270
C-O Alcohol (Stretching)	1135	1130	1125	1150
C-O Eter (Stretching)	1031	1050	-	1040

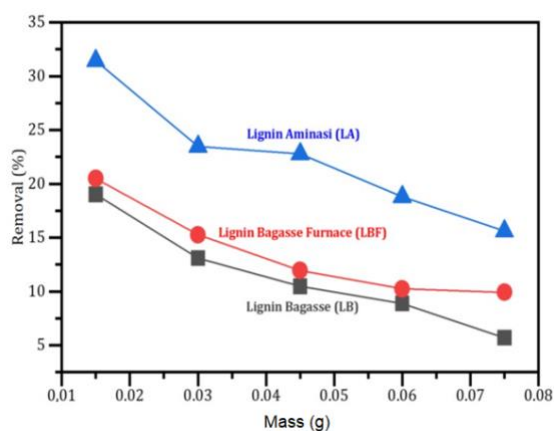


**Figure 1.** Graph of the Relationship between Mass Variations of LB, LBF, and LA adsorbents with 60 ppm Cr(III)

Analyzing the adsorption ability of bagasse lignin (LB), bagasse lignin carbon (LBF), and amination lignin (LA) as an adsorbent, with Cr(III) solution as an adsorbed species. Different testing variables, such as the mass variation test, contact time variation, and pH variation, would be utilized to evaluate the adsorption ability. The adsorption ability test has begun with varying the mass of the adsorbent to determine the optimum mass of each adsorbent LB, LBF, and LA against the Cr(III) adsorbate in the Figure 1.

Based on the experimental results seen from the percent removal value, it is possible to conclude that the absorption of Cr(III) adsorbate by lignin adsorbent is better by LA > LBF > LB. Carbonization and amination reaction in bagasse lignin has higher absorption than bagasse lignin



Isolation (LB). The carbonization process can open the surface pores of the lignin so that the surface area is larger and the absorption is higher. Then the presence of amination synthesis treatment (nitrogen group) can increase the adsorption capacity of metals and has good performance as an adsorption agent because nitrogen-containing bases are favored to form chelates with metal ions. The optimum mass for the three types of lignin adsorbents (LB, LBF, and LA) was 0.015 g as seen from the high percent removal. Increasing the amount of adsorbent can increase the effect of aggregation or the less active sites that can be used. The optimum mass gain of this adsorbent will then be used as a reference for testing other variations.

After testing the mass variation and obtaining the optimum mass, the contact time variation with the optimum mass was evaluated. The purpose of this experiment was to determine the optimal contact time for the three types of lignin adsorbents (LB, LBF, and LA) on Cr(III) adsorbate absorption. The optimum contact time is selected from the highest percent removal rate. The following **Figure 2** is the result of the adsorption ability test using variations in contact time on the three types of lignin samples.

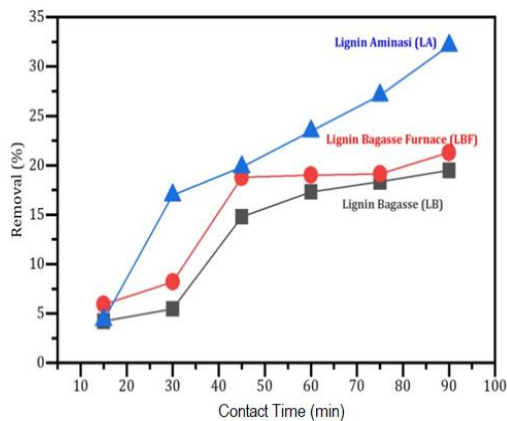


**Figure 2.** Graph of the Relationship of Contact Time Variations on LB, LBF, and LA adsorbents with 60 ppm Cr(III).

Based on the picture above, the optimum contact time for the three types of lignin (LB, LBF, and LA) was at a contact time of 90 minutes. This shows that the longer the contact time used, the greater the percent removal value. According to research published in 2011 by Isna Syauqiah et al. the longer the contact time employed, the longer the interaction between the adsorbate and the adsorbent, resulting in increased adsorbent

absorption or adsorption [24]. In addition, for the three types of adsorbents, the increase in percent removal along with the increase in contact time continued to increase from a predetermined contact time of 90 minutes. This is because the active sites in the three types of lignin (LB, LBF, and LA) have not reached saturation at 90 minutes.

In the pH variation test, the mass of the adsorbent and the optimum contact duration achieved in the previous test was employed. This pH variation test was conducted to determine the optimum pH of the adsorbate or Cr(III) solution because the pH value plays an essential role in the adsorption of heavy metal ions. The following **Figure 3** is the result of the adsorption ability test using variations in the pH of the Cr(III) adsorbate on the three types of lignin samples.

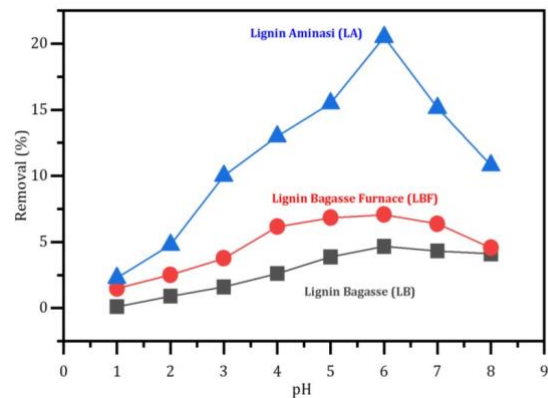
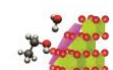


**Figure 3.** Graph of the Relationship of Variations in pH to Adsorbents LB (ash), LBF (red), and LA (blue) with 60 ppm Cr(III).

The absorption efficiency of heavy metal Cr(III) was performed in the pH range of 1 to 8. Based on the figure above, it can be seen that for the three types of adsorbents at pH 1 to 5, the percent removal continued to increase, and the peak was completed at pH 6. So that at pH 6, it was stated as the optimum pH for Cr(III) adsorbate. Then, at neutral and alkaline pH, the percent removal value decreased again. This is because at low pH  $H_3O^+$  ions with higher concentrations will compete with heavy metal Cr(III) to occupy the active site in the adsorption process. In an acidic pH solution, there will be an excess of protons which causes a rejection between the surface of the adsorbent and heavy metal ions (adsorbate), so that the absorption or adsorption will decrease [25,26]. In addition, at neutral pH (pH 7) the absorption efficiency will tend to decrease. That is because, at neutral pH, the ions undergo a hydrolysis reaction, which



makes the situation unstable and reduces absorption. Then at alkaline pH, metal ions can form metal hydroxide deposits so that the absorption is difficult to determine [27].

### 3.2 Adsorption Kinetics

Adsorption kinetics describes an adsorption binding rate to changes in contact time from the reaction equation. Adsorption kinetics can define the efficiency of the adsorption process. The adsorption kinetics is influenced by the absorption reaction that occurs between the adsorbent and the adsorbate and the transfer of ions to the active adsorption site contained in the adsorbent. The adsorption kinetics in this study used two kinetic models, namely the first-order pseudo-kinetic model and the second-order pseudo-kinetic model. The first-order pseudo-kinetic model describes a reversible equilibrium between the liquid phase in the adsorbate and the solid phase in the adsorbent. Meanwhile, pseudo-second-order is a limiting adsorption rate by considering a chemical reaction that occurs, such as electrostatic interactions, complex formation, and chelation formation [27].

The determination of the adsorption kinetics model can be seen from the value of  $R^2$ . The value of  $R^2$  is obtained from the linear straight-line equation plotted between  $\log(Q_e - Q_t)$  against time (t) in the first-order pseudo-kinetic model. Meanwhile, the pseudo-second-order kinetic model is obtained from the linear straight-line equation between  $t/Q_t$  against time (t). From the two plots of the linear straight-line equation, the

coefficient of determination  $R^2$  will be obtained. The following is a summary of the results of the adsorption kinetics test in Table 2.

**Table 2.** Summary of Adsorption Kinetics Test Results

	LB	LBF	LA
Orde 1	$R^2 = 0.9345$	$R^2 = 0.8664$	$R^2 = 0.9773$
Orde 2	$R^2 = 0.3301$	$R^2 = 0.6533$	$R^2 = 0.2920$

The adsorption mechanism of Cr(III) on the three types of lignin adsorbents (LB, LBF, and LA) based on the image of the adsorption kinetics model and the summary of the  $R^2$  values above, shows that all three follow the pseudo-first-order adsorption kinetics model. This is because the Cr(III) will stick to the active site of the adsorbent and will form an active complex compound. In the pseudo-first-order adsorption kinetics model, it is also explained that the reaction rate will depend on one of the reacting substances.

#### 3.2.1 Adsorption Isotherm

The equation of the adsorption isotherm, which is a distribution process that occurs between a solid-phase adsorbent and a liquid-phase adsorbate, defines the adsorption process. The Freundlich adsorption isotherm and the Langmuir adsorption isotherm are the two most often utilized adsorption isotherms [28]. The following is a table of several adsorption isotherm parameters in Table 3.

**Table 3.** Parameter of Adsorption Isotherm of each Adsorbent

Adsorbent	Temperature (°C)	Langmuir			Freundlich		
		Qm (mg/g)	KL (L/mg)	$R^2$	1/n	$K_F$	$R^2$
Lignin Bagasse	25	0.5509	289.31	0.8747	2.9232	$1.67 \times 10^{-5}$	0.9202
	30	8.6050	2.25	0.8010	1.4359	$1.49 \times 10^{-2}$	0.9313
	35	0.8181	144.39	0.7816	2.2922	$1.74 \times 10^{-4}$	0.9908
	40	1.1507	68.34	0.8633	2.5766	$1.04 \times 10^{-4}$	0.9361
Lignin Bagasse Furnace	25	1.1922	60.76	0.8696	2.7160	$7.53 \times 10^{-5}$	0.9526
	30	9.8717	1.48	0.9070	1.5178	$1.55 \times 10^{-2}$	0.9490
	35	2.2242	19.77	0.9159	2.1633	$7.00 \times 10^{-4}$	0.9874
	40	3.0921	10.11	0.9347	2.1616	$1.00 \times 10^{-3}$	0.9300
Lignin Aminasi	25	4.2900	3.67	0.7694	2.7253	$4.49 \times 10^{-4}$	0.9862
	30	7.1684	1.53	0.8884	2.2740	$2.35 \times 10^{-3}$	0.9840
	35	9.9800	0.94	0.7364	1.9177	$7.93 \times 10^{-3}$	0.9847
	40	1.4568	27.56	0.6035	3.7459	$1.02 \times 10^{-5}$	0.9482



Based on the research data summarized in Table 3, shows the  $R^2$  value for the three types of adsorbents which have a value closer to 1, namely the Freundlich isotherm equation model. The Freundlich isotherm model of the adsorption of Cr(III) on the three types of lignin adsorbents (LB, LBF, and LA) shows that the adsorption occurs in multilayer and the surface is heterogeneous or each active group on the surface of the adsorbent has different binding energy. The Freundlich adsorption isotherm equation in this test also allows the adsorbate to move freely so that the adsorption process that takes place occurs in many adsorption layers [29].

### 3.2.2 Adsorption Thermodynamics

The adsorption thermodynamics was carried out by testing the lignin adsorbent against Cr(III) using temperature variations. The temperatures used are 25°C, 30°C, 35°C, and 40°C. The thermodynamic parameters to be determined in this study are the value of Gibbs's free energy

( $\Delta G^\circ$ ), enthalpy value ( $\Delta H^\circ$ ), and entropy value ( $\Delta S^\circ$ ). Meanwhile, the determination of the enthalpy ( $\Delta H^\circ$ ) and entropy ( $\Delta S^\circ$ ) values is carried out by plotting a linear curve graph between  $\ln K$  on the y-axis to  $1/T$  on the y-axis. x. From the results of plotting the graph of the linear curve, it will be obtained the value of the equation of a straight line can be used to determine the value of enthalpy ( $\Delta H^\circ$ ) and entropy ( $\Delta S^\circ$ ).

Based on Table 4. the thermodynamics of Cr(III) adsorption by the three types of lignin adsorbents (LB, LBF, and LA) three have negative Gibbs free energy ( $\Delta G^\circ$ ). This value indicates that the reaction that occurs between the Cr(III) and the lignin adsorbent can run spontaneously. Then the enthalpy value ( $\Delta H^\circ$ ) for the adsorbents of bagasse lignin (LB) and bagasse lignin carbon (LBF) is positive, while amination lignin (LA) is negative. The difference in enthalpy value indicates the different strengths of the interaction between the metal ion Cr and each lignin adsorbent.

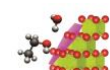
**Table 4.** Thermodynamic Parameters

Adsorbent	Temperature (K)	Thermodynamic Parameters		
		$\Delta G^\circ$ kJ/mol	$\Delta H^\circ$ kJ/mol	$\Delta S^\circ$ J/molK
Sugarcane Bagasse Lignin	298	-50.90	4.71	140.81
	303	-39.52		
	308	-50.82		
	313	-49.70		
Sugarcane Bagasse Lignin Carbon	298	-47.03	44.81	-2.69
	303	-38.46		
	308	-45.73		
	313	-44.73		
Amination Lignin	298	-40.08	-83.96	408.96
	303	-38.54		
	308	-37.93		
	313	-47.34		

Based on their enthalpy values, LB and LBF undergo an endothermic adsorption process with an adsorption mechanism by physisorption, this is because they have enthalpy values below 40 kJ/mol [30]. Meanwhile, LA-based on its enthalpy value undergoes an exothermic adsorption process with a chemisorption adsorption mechanism, and this is because its enthalpy value is in the range of 83-830 kJ/mol.

The entropy value ( $\Delta S^\circ$ ) for bagasse lignin (LB) and amination lignin (LA) is positive, and this indicates that the level of disorder in the solid-liquid adsorption system between adsorbent and

adsorbate has increased. The increase in the entropy value can be caused by the number of water molecules transferred so that a lot of entropy is translated rather than lost by Cr(III) which results in increased randomness at the solid/solution interface. The positive entropy value ( $\Delta S^\circ$ ) also indicates that the adsorption process is driven by entropy rather than enthalpy [31]. Meanwhile, bagasse lignin carbon (LBF) has a negative entropy value. This indicates that irregularities occur during the adsorption process caused by Cr(III) adsorbed by bagasse lignin



carbon (LBF), thereby reducing the freedom or the system becomes orderly.

#### 4 Conclusion

The ability of lignin adsorbents (LB, LBF, and LA) to adsorb Cr(III) resulted in optimum conditions at an adsorbent mass of 0.015 g, a contact time of 90 minutes, and the adsorbate solution had a pH of 6. The value of adsorption capacity ( $Q_m$ ) for bagasse lignin adsorbent (LB) was 8.6050 mg/g at 30 °C, bagasse carbon lignin (LBF) was 9.8717 mg/g at 30 °C, and amination lignin (LA) was 9.9800 mg/g at 35 °C. (aminated is more). The Cr(III) adsorption isotherm model follows the Freundlich isotherm model, which shows that the Cr(III) adsorption occurs in multilayers and the surface is heterogeneous or each active group on the surface of the adsorbent has a different binding energy. the Cr(III) adsorption kinetics model follows pseudo-first-order kinetics. These findings suggest that Cr(III) will adhere to the adsorbent's active site, forming an active complex molecule. The thermodynamics of Cr(III) adsorption for bagasse lignin (LB) has a spontaneous reaction at high temperatures. Bagasse lignin carbon (LBF) has a spontaneous reaction at low temperatures. Meanwhile, aminated lignin (LA) has a spontaneous reaction at high temperatures.

#### Acknowledgment

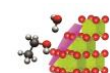
Thanks to Pertamina University for internal funding as well as related parties at the Materials and Energy Engineering Laboratory.

#### References

- [1] Sun, Y., Wang, T., Sun, X., Bai, L., Han, C. and Zhang, P. 2021. The potential of biochar and lignin-based adsorbents for wastewater treatment: Comparison, mechanism, and application—A review. *Industrial Crops and Products*, Elsevier BV. 166 113473. 10.1016/j.indcrop.2021.113473
- [2] Vakili, M., Rafatullah, M., Salamatinia, B., Abdullah, A.Z., Ibrahim, M.H., Tan, K.B. et al. 2014. Application of chitosan and its derivatives as adsorbents for dye removal from water and wastewater: A review. *Carbohydrate Polymers*, Elsevier BV. 113 115–30. 10.1016/j.carbpol.2014.07.007
- [3] Vardhan, K.H., Kumar, P.S. and Panda, R.C. 2019. A review on heavy metal pollution, toxicity and remedial measures: Current trends and future perspectives. *Journal of Molecular Liquids*, Elsevier BV. 290 111197. 10.1016/j.molliq.2019.111197
- [4] Rivas, B.L., Pereira, E.D., Palencia, M. and Sánchez, J. 2011. Water-soluble functional polymers in conjunction with membranes to remove pollutant ions from aqueous solutions. *Progress in Polymer Science*, Elsevier BV. 36 (2) 294–322. 10.1016/j.progpolymsci.2010.11.001
- [5] Sosa-Rodríguez, F.S., Vazquez-Arenas, J., Peña, P.P., Escobedo-Bretado, M.A., Castellanos-Juárez, F.X., Labastida, I. et al. 2020. Spatial distribution, mobility and potential health risks of arsenic and lead concentrations in semiarid fine top-soils of Durango City, Mexico. *CATENA*, Elsevier BV. 190 104540. 10.1016/j.catena.2020.104540
- [6] Xiao, X., Zhang, J., Wang, H., Han, X., Ma, J., Ma, Y. et al. 2020. Distribution and health risk assessment of potentially toxic elements in soils around coal industrial areas: A global meta-analysis. *Science of The Total Environment*, Elsevier BV. 713 135292. 10.1016/j.scitotenv.2019.135292
- [7] Chowdhury, S., Mazumder, M.A.J., Al-Attas, O. and Husain, T. 2016. Heavy metals in drinking water: Occurrences, implications, and future needs in developing countries. *Science of The Total Environment*, Elsevier BV. 569–570 476–88. 10.1016/j.scitotenv.2016.06.166
- [8] Qin, Y., Wang, L., Zhao, C., Chen, D., Ma, Y. and Yang, W. 2016. Ammonium-Functionalized Hollow Polymer Particles As a pH-Responsive Adsorbent for Selective Removal of Acid Dye. *ACS Applied Materials & Interfaces*, American Chemical Society (ACS). 8 (26) 16690–8. 10.1021/acsami.6b04199
- [9] Chen, J.P. 2013. Decontamination of Heavy Metals: Processes, Mechanisms,



- and Applications. 1st editio. CRC Press. 10.1201/b12672
- [10] Qin, H., Hu, T., Zhai, Y., Lu, N. and Aliyeva, J. 2020. The improved methods of heavy metals removal by biosorbents: A review. *Environmental Pollution*, Elsevier BV. 258 113777. 10.1016/j.envpol.2019.113777
- [11] Wang, X. 2012. Nanomaterials as Sorbents to Remove Heavy Metal Ions in Wastewater Treatment. *Journal of Environmental & Analytical Toxicology*, OMICS Publishing Group. 02 (07). 10.4172/2161-0525.1000154
- [12] Chen, H., Zhong, A., Wu, J., Zhao, J. and Yan, H. 2012. Adsorption Behaviors and Mechanisms of Methyl Orange on Heat-Treated Palygorskite Clays. *Industrial & Engineering Chemistry Research*, American Chemical Society (ACS). 51 (43) 14026–36. 10.1021/ie300702j
- [13] Li, J., Xing, X., Li, J., Shi, M., Lin, A., Xu, C. et al. 2018. Preparation of thiol-functionalized activated carbon from sewage sludge with coal blending for heavy metal removal from contaminated water. *Environmental Pollution*, Elsevier BV. 234 677–83. 10.1016/j.envpol.2017.11.102
- [14] Salihi, I.U., Kuty, S.R.M. and Ismail, H.H.M. 2018. Copper Metal Removal using Sludge Activated Carbon Derived from Wastewater Treatment Sludge. *MATEC Web of Conferences*, EDP Sciences. 203 3009. 10.1051/mateconf/201820303009
- [15] Musarurwa, H. and Tavengwa, N.T. 2020. Application of carboxymethyl polysaccharides as bio-sorbents for the sequestration of heavy metals in aquatic environments. *Carbohydrate Polymers*, Elsevier BV. 237 116142. 10.1016/j.carbpol.2020.116142
- [16] Santander, P., Butter, B., Oyarce, E., Yáñez, M., Xiao, L.-P. and Sánchez, J. 2021. Lignin-based adsorbent materials for metal ion removal from wastewater: A review. *Industrial Crops and Products*, Elsevier BV. 167 113510. 10.1016/j.indcrop.2021.113510
- [17] Chung, H. and Washburn, N.R. 2013. Chemistry of lignin-based materials. *Green Materials*, Thomas Telford Ltd. 1 (3) 137–60. 10.1680/gmat.12.00009
- [18] Thakur, V.K., Thakur, M.K., Raghavan, P. and Kessler, M.R. 2014. Progress in Green Polymer Composites from Lignin for Multifunctional Applications: A Review. *ACS Sustainable Chemistry & Engineering*, American Chemical Society (ACS). 2 (5) 1072–92. 10.1021/sc500087z
- [19] Naseer, A., Jamshaid, A., Hamid, A., Muhammad, N., Ghauri, M., Iqbal, J. et al. 2018. Lignin and Lignin Based Materials for the Removal of Heavy Metals from Waste Water-An Overview. *Zeitschrift Für Physikalische Chemie*, Walter de Gruyter GmbH. 233 (3) 315–45. 10.1515/zpch-2018-1209
- [20] Ge, Y., Li, Z., Kong, Y., Song, Q. and Wang, K. 2014. Heavy metal ions retention by bi-functionalized lignin: Synthesis, applications, and adsorption mechanisms. *Journal of Industrial and Engineering Chemistry*, Elsevier BV. 20 (6) 4429–36. 10.1016/j.jiec.2014.02.011
- [21] Al Arni, S. (2018). Extraction and isolation methods for lignin separation from sugarcane bagasse: a review. *Industrial Crops and Products*, 115, 330-339.
- [22] Moubarik, A., Grimi, N., Boussetta, N. and Pizzi, A. 2013. Isolation and characterization of lignin from Moroccan sugar cane bagasse: Production of lignin-phenol-formaldehyde wood adhesive. *Industrial Crops and Products*, Elsevier BV. 45 296–302. 10.1016/j.indcrop.2012.12.040
- [23] Pari, G., Sofyan, K., Syafii, W., Buchari, B. and Yamamoto, H. 2006. Kajian Struktur Arang dari Lignin. *Jurnal Penelitian Hasil Hutan*, National Research



- and Innovation Agency. 24 (1) 9–20. 10.20886/jphh.2006.24.1.9-20
- [24] Syauqiah, I., Amalia, M. and Kartini, H.A. 2011. Analisis Variasi Waktu dan Kecepatan Pengaduk pada Proses Adsorpsi Limbah Logam Berat dengan Arang Aktif. *Info Teknik: Jurnal Keilmuan Dan Aplikasi Teknik*, 12 (1) 11–20.
- [25] Laus, R. and de Fávère, V.T. 2011. Competitive adsorption of Cu(II) and Cd(II) ions by chitosan crosslinked with epichlorohydrin–triphosphate. *Bioresource Technology*, Elsevier BV. 102 (19) 8769–76. 10.1016/j.biortech.2011.07.057
- [26] Liu, Y., Shen, X., Xian, Q., Chen, H., Zou, H. and Gao, S. 2006. Adsorption of copper and lead in aqueous solution onto bentonite modified by 4'-methylbenzo-15-crown-5. *Journal of Hazardous Materials*, Elsevier BV. 137 (2) 1149–55. 10.1016/j.jhazmat.2006.03.057
- [27] Liu, Y., Shen, X., Xian, Q., Chen, H., Zou, H. and Gao, S. 2006. Adsorption of copper and lead in aqueous solution onto bentonite modified by 4'-methylbenzo-15-crown-5. *Journal of Hazardous Materials*, 137 (2) 1149–55. 10.1016/j.jhazmat.2006.03.057
- [28] Kusuma, I.D.G.D.P., Wiratini, N.M. and Wiratma, I.G.L. 2017. Isoterm Adsorpsi Cu<sup>2+</sup> oleh Biomassa Rumput Laut *Eucheuma Spinosum*. *Jurnal Pendidikan Kimia Undiksha*, 1 (1). 10.23887/jjpk.v1i1.3524
- [29] Sari Rensy Aula, M. Lutfi Firdaus and Elvia Rina. 2017. Penentuan Kesetimbangan, Termodinamika Dan Kinetika Adsorpsi Arang Aktif Tempurung Kelapa Sawit Pada Zat Warna Reactive Red Dan Direct Blue. *Alotrop*, 1 (1) 10–4.
- [30] Yang, J., Yu, M. and Qiu, T. 2014. Adsorption thermodynamics and kinetics of Cr(VI) on KIP210 resin. *Journal of Industrial and Engineering Chemistry*, The Korean Society of Industrial and Engineering Chemistry. 20 (2) 480–6. 10.1016/j.jiec.2013.05.005
- [31] El-Moselhy, K., Abdel Azzem, M., Amer, A. and Al-Prol, A. 2017. Adsorption of Cu(II) and Cd(II) from aqueous solution by using rice husk adsorbent. *Physical Chemistry: An Indian Journal*, 12 109–22.

